

filters using dual-mode cross-slotted square resonators, J Supercond Incomp Novel Magnetism 14 (2000), 131–137.

8. M.G. Banciu, R. Ramer, and A. Ioachim, Compact microstrip resonators for 900 MHz, IEEE Microwave Wireless Compon Lett 13 (2003), 175–177.
9. A. Ioachim, M.G. Banciu, M.I. Toacsan, et. al., Nickel-doped ($\text{Zr}_{0.8}\text{Sn}_{0.2}\text{TiO}_4$) for microwave and millimeter-wave applications, Mater Sci Eng B 118 (2005), 205–209.

© 2007 Wiley Periodicals, Inc.

MEASUREMENT AND ANALYSIS OF OPTICAL PARAMETERS IN ANISOTROPIC SLAB ONE-SIDE LEAKY WAVEGUIDES

Fubin Gao,¹ Guotong Du,¹ Yuan Sun,¹ and Ping Zhang²

¹ State Key laboratory on Integrated Opto-electronics, College of Electronic Science and Engineering, Jilin University, Changchun 130012, China

² State Key Lab of Applied Optics, Changchun Institute of Optics, Fine Mechanics and Physics, Chinese Academy of Sciences, Changchun 130033, China

Received 1 February 2007

ABSTRACT: Leaky modes of anisotropic slab one-side leaky waveguides have been analyzed, and an efficient method for measuring optical parameters of these waveguides is presented in this article by using the prism coupling technique. Measured results show that errors of the refractive indices are within 2.1×10^{-4} . © 2007 Wiley Periodicals, Inc. Microwave Opt Technol Lett 49: 2295–2299, 2007; DOI 10.1002/mop.22721

Key words: anisotropic slab one-side leaky waveguide; optical parameters; prism coupling technique; measurement and analysis

1. INTRODUCTION

Among many optical waveguide devices, the optical anisotropy of waveguides is an important property. For example, for optical splitters, combiners, wavelength-division multiplexers/demultiplexers (WDM) with arrayed waveguide grating (AWG) and multi-interferometer couplers (MMI), their waveguides have no or very low optical anisotropy. On the other hand, for optical waveguide electro-optic modulators and polarizers, their waveguides have higher optical anisotropy. Therefore, how to measure the property of their optical anisotropy is very important for the design and fabrication of the devices. Ellipsometry and spectroscopic ellipsometry can be used to measure the index and thickness of isotropy waveguide films, but the method cannot be used for anisotropy waveguide films. The prism coupling technique [1] is another efficient method for measuring index and thickness of waveguide films in the field of integrated optics. Up to now, there have been many reports [2–4] about measuring the index of waveguides, but they all were used to measure isotropy waveguides and were studied on only one polarization. For characterizing anisotropy of waveguides, we have reported a guided-mode method for measuring electro-optic coefficients of poled polymer waveguides [5]. During developing the polymer waveguide devices, we have presented an efficient method for measuring the parameters of single-mode anisotropic slab waveguides [6]. It is necessary to measure waveguide parameters expediently and effectively in the study because the stability of polymer materials is not as good as that of inorganic materials. Generally, refractive indices of polymer materials are very low so

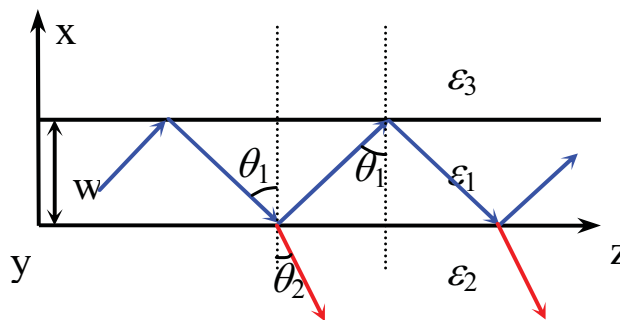


Figure 1 Zigzag path of a ray as a leaky mode in the one-side leaky waveguide. [Color figure can be viewed in the online issue, which is available at www.interscience.wiley.com]

that the selection range of substrate refractive indices for forming real waveguides is very narrow. In addition, the waveguides with small difference of indices between polymer waveguide layers and substrates cannot form enough guided modes for measuring the waveguide index and thickness by using the guided mode method, whereas, for one-side leaky waveguides, the selection range of substrates indices is so wide that they can form enough leaky modes.

In this article, leaky modes of polymer one-side leaky waveguides have been measured by using the prism coupling technique in all different phase shift regions. The measuring results have been analyzed carefully. Based on leaky modes, the parameters of the waveguides have been solved from the leaky mode anisotropic characteristic equation. In the measurement, we have observed the phase change at the Brewster's angle for TM modes. The measuring method and data treatment can be used to obtain the polymer waveguide parameters with higher precision.

2. CHARACTERISTIC EQUATIONS OF ANISOTROPIC SLAB ONE-SIDE LEAKY WAVEGUIDES

The waveguide treated here is a two-dimensional structure consisting of three layers; the substrate, the film, and the top layer. Materials are all assumed lossless. In the principal coordinate system, the relative dielectric tensors $[\varepsilon]$ is given by [7]

$$[\varepsilon] = \begin{bmatrix} \varepsilon_{xx} & 0 & 0 \\ 0 & \varepsilon_{yy} & 0 \\ 0 & 0 & \varepsilon_{zz} \end{bmatrix}, \quad (1)$$

where x -axis is normal to the plane of slab waveguides, z -axis is the traveling direction of the lightwave in the waveguides, and y -axis is normal to the x – z plane.

Under this condition, the anisotropic characteristic equation for TE mode is shown as follows

$$\kappa_{1\text{TE}} w = m_{\text{TE}} \pi + \phi_{12\text{TE}} + \phi_{13\text{TE}}, \quad (m_{\text{TE}} = 0, 1, 2, \dots), \quad (2)$$

where m_{TE} is the mode order number for TE mode, $\phi_{12\text{TE}}$ and $\phi_{13\text{TE}}$ are the phase shifts occurring at 1–2 and 1–3 interfaces, respectively. $\kappa_{1\text{TE}}$ is the propagation constant in the x direction and expressed in terms of a propagation constant in the z direction β_{TE} and the free space propagation constant k_0 by

$$\kappa_{1\text{TE}}^2 = k_0^2 \varepsilon_{1yy} - \beta_{\text{TE}}^2, \quad (3)$$

When $\varepsilon_2 > \varepsilon_1 \geq \varepsilon_3$, three layers form of one-side leaky waveguides as shown in Figure 1. Because the angle of incidence

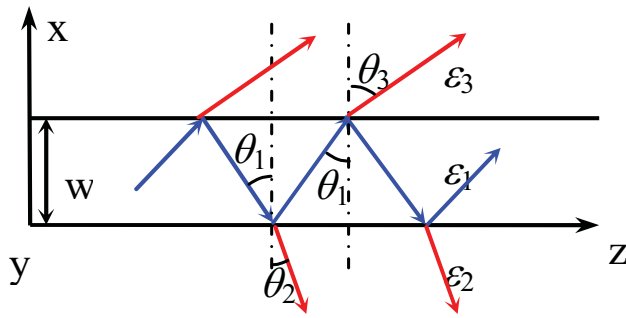


Figure 2 Zigzag path of a ray as a leaky mode in the two-side leaky waveguide. [Color figure can be viewed in the online issue, which is available at www.interscience.wiley.com]

θ_1 is always greater than θ_2 , ϕ_{12TE} is always equal to $\pi/2$ in the region $\pi/2 > \theta_1 > 0$.

The expression of ϕ_{13TE} depends on the value of the angle of incidence θ_1 of the TE-polarized light propagating in the film.

In the region $\theta_1 > \theta_{13c}$ (θ_{13c} is the critical angle at 1–3 interface), the ray suffers total internal reflection at the 1–3 interface and partial internal reflection at the 1–2 interface, as shown in Figure 1. This leads to a series of discrete modes called leaky waves in the substrate radiation mode regime.

Then, when $\theta_1 < \theta_{13c}$, the ray suffers partial internal reflection at both interfaces, as shown in Figure 2. We obtain a series of discrete modes, which lead to leaky waves in the cladding radiation mode regime. These modes leak both into the substrate and into the cladding. Therefore, the phase shifts at the 1–2 and 1–3 interfaces are respectively given by

$$\phi_{12TE} = \frac{\pi}{2}, \quad (4)$$

$$\phi_{13TE} = \begin{cases} \tan^{-1}(q_{TE}/\kappa_{1TE}), & \theta_1 \geq \theta_{13c} \\ \pi/2, & \theta_1 < \theta_{13c} \end{cases} \quad (5)$$

$$q_{TE}^2 = \beta_{mTE}^2 - k_0^2 \epsilon_{3yy}, \quad (6)$$

Similarly, the anisotropic characteristic equation for TM mode is shown as follows

$$\kappa_{1TM} w = m_{TM} \pi + \phi_{12TM} + \phi_{13TM}, \quad (m_{TM} = 0, 1, 2, \dots), \quad (7)$$

$$\kappa_{1TM}^2 = \frac{\epsilon_{1zz}}{\epsilon_{1xx}} (k_0^2 \epsilon_{1xx} - \beta_{mTM}^2), \quad (8)$$

In the case of $\epsilon_2 > \epsilon_1 \geq \epsilon_3$, $\phi_{12TM} = \pi/2$ and the expressions of ϕ_{13TM} depend on the value of the angle of incidence θ_1 of the TM-polarized light propagating in the film.

We consider the phase shift occurring at the 1–3 interface. First, if $\theta_1 > \theta_{13c}$, the ray suffers total internal reflection, and ϕ_{12TM} is the phase shifts of total internal reflection. Second, in the region $\theta_{13c} > \theta_1 > \theta_{13p}$ (θ_{13p} is Brewster's angle at the 1–3 interface), the ray suffers partial internal reflection, and $\phi_{12TM} = 0$ derived from Fresnel formulae [8]. Third, when $\theta_1 < \theta_{13p}$, the ray also suffers partial internal reflection, but $\phi_{12TM} = \pi/2$ derived from Fresnel formulae [8], too.

Therefore, the phase shifts at the 1–2 and 1–3 interfaces are respectively given by

$$\phi_{12TM} = \begin{cases} 0 & \theta_1 \geq \theta_{12p} \\ \frac{\pi}{2}, & \theta_1 < \theta_{12p} \end{cases}, \quad (9)$$

$$\phi_{13TM} = \begin{cases} \tan^{-1}\left(\frac{\epsilon_{1zz}}{\epsilon_{3zz}} \frac{q_{TM}}{\kappa_{1TM}}\right), & \theta_1 \geq \theta_{13c} \\ 0, & \theta_{13p} \leq \theta_1 < \theta_{13c}, \\ \frac{\pi}{2}, & \theta_1 < \theta_{13p} \end{cases} \quad (10)$$

$$q_{TM}^2 = \frac{\epsilon_{3zz}}{\epsilon_{3xx}} (\beta_{mTM}^2 - k_0^2 \epsilon_{3xx}). \quad (11)$$

3. MODEL AND PARAMETERS OF WAVEGUIDES

The waveguide studied here is made up of the isotropic substrate, the isotropic top layer but the uniaxial-guided layer. The term of dielectric tensor of the substrate is

$$\epsilon_{2xx} = \epsilon_{2yy} = \epsilon_{2zz} = n_b^2, \quad (12)$$

and the term of dielectric tensor of the top layer is

$$\epsilon_{3xx} = \epsilon_{3yy} = \epsilon_{3zz} = n_c^2, \quad (13)$$

where n_b and n_c are the substrate and the top layer refractive indices, respectively.

The refractive index ellipsoid of the uniaxial-guided layer is a uniaxial ellipsoid as shown in Figure 3. Hence, the terms of dielectric tensor are

$$\epsilon_{1xx} = n_e^2, \quad \epsilon_{1yy} = \epsilon_{1zz} = n_o^2, \quad (14)$$

where n_e and n_o are called the unordinary refractive index parallel to the x -axis and the ordinary refractive index in the y - z plane, respectively. For the one-side leaky waveguide, $n_b > n_e$, $n_o > n_c$.

The propagation constants for TE and TM modes in z direction are expressed by

$$\beta_{mTE} = k_0 N_{mTE}, \quad \beta_{mTM} = k_0 N_{mTM} \quad (15)$$

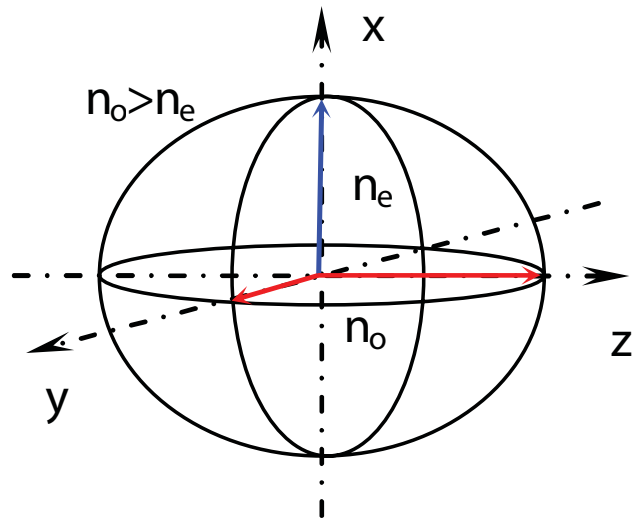


Figure 3 The refractive index ellipsoid of the uniaxial-guided layer. [Color figure can be viewed in the online issue, which is available at www.interscience.wiley.com]

where N_{mTE} and N_{mTM} are TE and TM modes effective refractive indices, respectively.

Substituting Eqs. (12)–(15) into Eqs. (2)–(11), we obtain

$$wk_0\sqrt{n_o^2 - N_{mTE}^2} = m_{TE}\pi + \phi_{12TE} + \phi_{13TE}, \quad (m_{TE} = 0, 1, 2, \dots), \quad (16)$$

$$\phi_{12TE} = \frac{\pi}{2}, \quad (17)$$

$$\phi_{13TE} = \begin{cases} \tan^{-1} \frac{\sqrt{N_{mTE}^2 - n_c^2}}{\sqrt{n_o^2 - N_{mTE}^2}}, & N_{mTE} \geq n_c, \\ \pi/2, & N_{mTE} < n_c \end{cases}, \quad (18)$$

$$wk_0 \frac{n_o}{n_c} \sqrt{n_c^2 - N_{mTM}^2} = m_{TM}\pi + \phi_{12TM} + \phi_{13TM}, \quad (m_{TM} = 0, 1, 2, \dots), \quad (19)$$

$$\phi_{12TM} = \begin{cases} 0, & N_{mTM} \geq N_{12p} \\ \frac{\pi}{2}, & N_{mTM} < N_{12p} \end{cases}, \quad (20)$$

$$\phi_{13TM} = \begin{cases} \tan^{-1} \left(\frac{n_o n_e \sqrt{N_{mTM}^2 - n_c^2}}{n_c^2 \sqrt{n_e^2 - N_{mTM}^2}} \right), & N_{mTM} \geq n_c \\ 0, & N_{13p} < N_{mTM} < n_c, \\ \frac{\pi}{2}, & N_{mTM} < N_{13p} \end{cases} \quad (21)$$

where N_{12p} and N_{13p} are the TM mode effective refractive indices related to the *Brewster's angle* θ_{12p} and θ_{13p} at the 1–2 and 1–3 interfaces, respectively by

$$N_{12p} = n_{13p} \sin(\theta_{12p}), \quad N_{13p} = n_{13p} \sin(\theta_{13p}), \quad (22)$$

where n_{12p} and n_{13p} are the real refractive indices related the *Brewster's angle* θ_{12p} and θ_{13p} at the 1–2 and 1–3 interfaces, respectively. According to *Brewster's law*

$$\theta_{12p} = \tan\left(\frac{n_b}{n_{12p}}\right), \quad \theta_{13p} = \tan\left(\frac{n_c}{n_{13p}}\right) \quad (23)$$

For the TM-polarized light, the index ellipse in the incident plane is shown in Figure 4, and its equation is

$$\frac{n_i^2 \cos^2 \theta_i}{n_o^2} + \frac{n_i^2 \sin^2 \theta_i}{n_e^2} = 1 \quad (24)$$

When $\theta_i = \theta_{12p}$ and $\theta_i = \theta_{13p}$ respectively, n_{12p} and n_{13p} can be solved from Eqs. (23) and (24) as shown below

$$n_{12p} = \frac{2n_e n_o n_o}{\sqrt{2n_o(n_o n_b^2 + \sqrt{n_o^2 n_c^4 - 2n_o^2 n_c^2 n_b^2 + n_o^2 n_b^4 + 4n_b^2 n_b^4 - n_o n_c^2})}} \quad (25)$$

$$n_{13p} = \frac{2n_e n_o n_c}{\sqrt{2n_o(n_o n_c^2 + \sqrt{n_o^2 n_c^4 - 2n_o^2 n_c^2 n_c^2 + n_o^2 n_c^4 + 4n_c^2 n_c^4 - n_o n_c^2})}} \quad (26)$$

When $0 < \theta_i < \pi/2$, $n_o > n_i > n_e$. For many anisotropic materials used in optical waveguide devices, the difference of n_o and n_e is very small, so that n_i in Eq. (25) can be replaced by n_e .

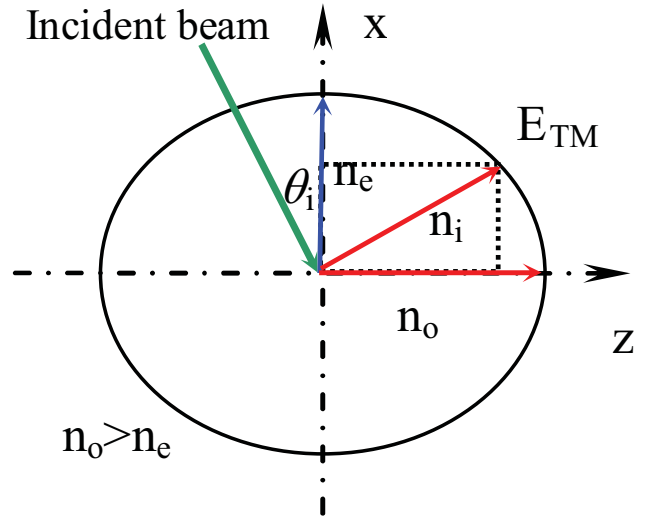


Figure 4 Refractive index ellipse in the x - z plane. [Color figure can be viewed in the online issue, which is available at www.interscience.wiley.com]

4. MEASUREMENT AND DATA TREATMENT

As we know, the mode effective refractive index N_m can be measured by the prism coupling technique [1]. The relationship between the mode effective refractive index N_m and the synchronous angles α_m can be described as follows

$$N_m = \sin \alpha_m \cos \alpha_p + \sin \alpha_p \sqrt{n_p^2 - \sin^2 \alpha_m}, \quad (m = 0, 1, 2, \dots) \quad (27)$$

where $m = 0, 1, 2, \dots, n_p$, and α_p are the mode order number, the prism refractive index and angle, respectively. If the numbers of observed N_{mTE} and N_{mTM} are M_{TE} and M_{TM} , respectively, Eqs. (16) and (19) form an equation system involving $M_{TE} + M_{TM}$ transcendental equations about three unknown n_e , n_o , and w .

To find the unknown parameters n_e , n_o , and w , the objective function is defined as follows

$$S = \left[\sum_{m_{TE}=0}^{M_{mTE}-1} (\Delta N_{mTE})^2 + \sum_{m_{TM}=0}^{M_{mTM}-1} (\Delta N_{mTM})^2 \right]^{1/2} / (M_{mTE} + M_{mTM}), \quad (28)$$

$$\Delta N_{mTE} = N_{mTE} - N_{mTE0}(n_e, n_o, w),$$

$$\Delta N_{mTM} = N_{mTM} - N_{mTM0}(n_e, n_o, w) \quad (29)$$

where $N_{mTE0}(n_e, n_o, w)$ and $N_{mTM0}(n_e, n_o, w)$ are the theoretical values of N_{mTE} and N_{mTM} . For the given values of n_e , n_o , and w , N_{mTE0} and N_{mTM0} can be found from Eqs. (16) and (19) by a numerical method with a computer.

We can adjust the unknown parameters n_e , n_o , and w until S approaches minimum as closely as possible. We regard those parameters n_{e0} , n_{o0} , and w_0 , for which S is equal to the minimum S_{min} , as the measured values of n_e , n_o , and w . The measured error is S_{min} .

5. RESULTS AND DISCUSSION

A sample was made by spin-coating PMMA polymer solution on a single-crystal silicon substrate at a certain rotate speed. Then it was solidified at 120°C over 3 h. The reason for selecting single-

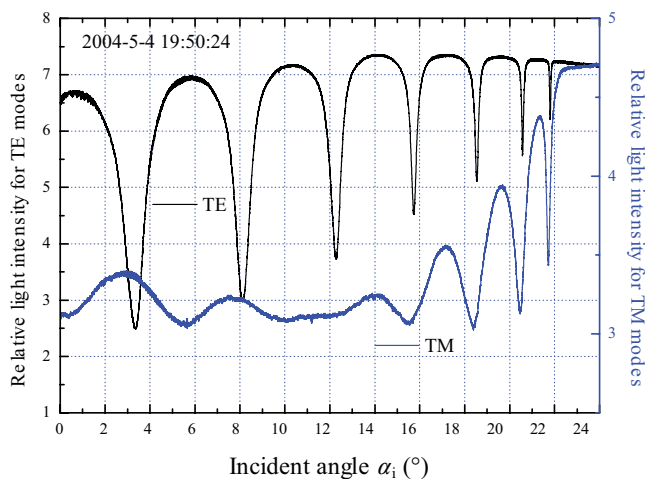


Figure 5 Curves of relative light intensity varying the incidence angle for the PMMA polymer film. [Color figure can be viewed in the online issue, which is available at www.interscience.wiley.com]

crystal silicon as the substrate is that it has greater refractive index, so that almost all transparent medium films based on silicon can form one side leaky waveguides with enough leaky modes.

We also used the measurement system described in Ref. [6]. In the measurement, n_p and α_p of a symmetrical glass prism are 1.79785 and 44.9944°, respectively. The refractive indices of the top layer (air) and substrate are the 1.0000 and 3.85593 – 0.02i, respectively, at 650-nm wavelength. Since the real part of the effective refractive index for Si is much greater than its imaginary part, the imaginary part was neglected in our data treatment. In fact, for one-side leaky waveguides, n_b does not appear in their mode characteristic Eqs. (16) and (19), so that the quantity of n_b does not affect the calculating result.

The leaky waveguide sample was measured and both curves of relative light intensity output from the prism varying with the incident angle for TE and TM modes are shown in Figure 5. According to the positions of negative peaks in Figure 5, the values of the synchronous angles for both TE and TM modes are obtained and listed in Table 1. The polymer waveguide parameters have been calculated with our MATLAB programs and the calculating results are listed in Table 1, too. According to the results, n_e and n_o are 1.50986 and 1.50976, respectively. Because n_e and n_o are equal in the range of the measurement error, it indicates that PMMA polymer waveguide film is isotropic.

The Brewster's angle θ_{12p} and relative incident angle α_{12p} at 1–2 interface are 68.6164° and 11.6505°, respectively. As shown in Figure 5, we have measured the phase change of $\pi/2$ when α_i is equal to α_{12p} for the TM mode. For verifying the correctness of our characteristic equations, we used the effective refractive indices of

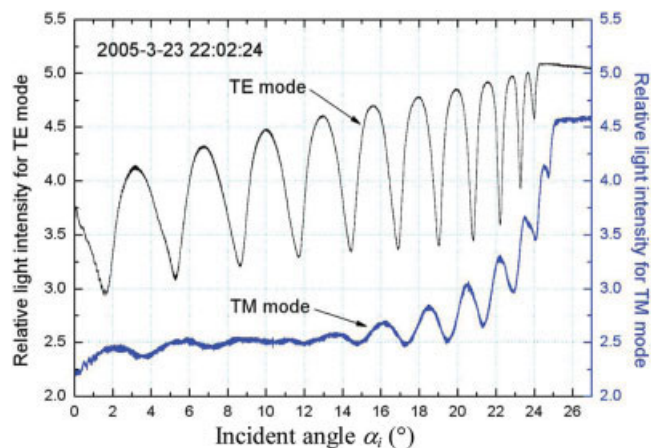


Figure 6 Curves of relative light intensity varying the incidence angle for the poled DR1 polymer film. [Color figure can be viewed in the online issue, which is available at www.interscience.wiley.com]

the 6th and 7th modes for TM mode in the calculation, and got high precision results.

For testifying the validity of our method applied to measure anisotropic leaky waveguide films, we have measured the sample of poled DR1 polymer film on the silicon substrate. The curves of output light intensity varying with the incident angle for TE and TM modes are shown in Figure 6. The calculated results are listed in Table 2. Because the sample had been corona poled before the measurement, n_e is greater than n_o . This measuring result indicates that poled DR1 polymer waveguide film is monaxial anisotropic.

About error problem, one of the reasons bring errors is that determining reference angle, equivalent to the table position where the incident beam is perpendicular to the face of the prism. In our measurement, we determine the reference angle by manual adjusting the table in order to the laser beam reflected from the incident face of the prism goes back to the incidence direction. The manual adjusting and identifying by eyes bring about the main random error. Another error originates from the determination of the position of the negative peak related to the leaky mode. Both these errors are artificial errors. In the solving process by computer program, we assume that the computing error of independent variables is equal to 1×10^{-5} , and the computing error of the function of the mode characterized equation is equal to 1×10^{-5} . In practice, the synthesis error is equal to 2×10^{-4} , so we can consider that the artificial error is dominating and the computing errors can be neglected.

6. CONCLUSION

We have presented the characteristic equations of one-side leaky modes being same with all leaky mode ranges. Especially, the

TABLE 1 Measured Data and Calculated Results for the PMMA Polymer Film

m_{TE}	a_{mTE} (°)	N_{mTE}	N_{mTE0}	ΔN_{mTE} (10^{-4})	m_{TM}	a_{mTM} (°)	N_{mTM}	N_{mTM0}	ΔN_{mTM} (10^{-4})
0	21.7972	1.50633	1.50600	3.3	0	21.7238	1.50567	1.50596	–2.9
1	20.5909	1.49530	1.49464	6.6	1	20.4650	1.49413	1.49420	–0.7
2	18.5350	1.47592	1.47556	3.6	2	18.4091	1.47471	1.47449	2.2
3	15.7448	1.44848	1.44848	0.0	3	15.4615	1.44562	1.44640	–7.8
4	12.2832	1.41266	1.41287	–2.1	6	5.5909	1.33818	1.33661	15.7
5	8.0874	1.36674	1.36827	–15.3	7	0.2727	1.27451	1.27476	–2.5
$\theta_{12p} = 68.6164^\circ$		$\alpha_{12p} = 11.6505^\circ$			$n_{o0} = 1.50976$		$w_o = 2.9588 \mu m$		
$\theta_{13p} = 33.5182^\circ$		$\alpha_{13p} = -32.4545^\circ$			$n_{e0} = 1.50986$		$S_{min} = 2.1 \times 10^{-4}$		

TABLE 2 Measured Data and Calculated Results for the Poled DR1 Polymer Film

m_{TE}	a_{mTE} (°)	N_{mTE}	N_{mTE0}	ΔN_{mTE} (10^{-4})	m_{TM}	a_{mTM} (°)	N_{mTM}	N_{mTM0}	ΔN_{mTM} (10^{-4})
0	23.9934	1.52577	1.52558	1.9	0	24.7598	1.53235	1.53190	4.5
1	23.2742	1.51950	1.51998	-4.8	1	24.0878	1.52658	1.52614	4.5
2	22.2131	1.51008	1.51067	-5.9	2	22.9323	1.51648	1.51656	-0.7
3	20.8218	1.49743	1.49750	-0.7	3	21.3524	1.50229	1.50303	-7.3
4	19.0415	1.48076	1.48047	2.9	4	19.4778	1.48490	1.48540	-5.1
5	16.8838	1.45984	1.45934	5.0	5	17.3201	1.46413	1.46370	4.3
$\theta_{12p} = 68.3200^\circ$		$\alpha_{12p} = 13.4034^\circ$			$n_{o0} = 1.52742$		$w_0 = 4.2315 \mu m$		
$\theta_{13p} = 33.1802^\circ$		$\alpha_{13p} = -32.2174^\circ$			$n_{e0} = 1.53377$		$S_{min} = 1.3 \times 10^{-4}$		

phase changes brought by *Brewster's angle* have been considered in the equations. By using our measurement setup, the optical parameters of an isotropic PMMA polymer waveguide film and an anisotropic poled DR1 polymer waveguide film have been measured. This method is suitable to measure the slab waveguide films with low refractive indices or anisotropy. For one side leaky waveguides, there is no n_b in their anisotropic characteristic equations, so that the selection range of the refractive index of the substrate is wide and does not need exact quantity. So this method is an excellent tool for the optical parameter measurement of most transparent medium films. Also, it is much helpful for the design and fabrication of optical waveguide devices. We are just considering applying this method for the measurement of Biochemical Sensing Applications.

ACKNOWLEDGMENT

This research was financially supported by the National Natural Science Foundation of China (Project No. 60274041). The authors gratefully acknowledge Dr. Alin Hou for her poled DR1 polymer film samples.

REFERENCES

1. R. Ulrich and R. Torge, Measurement of film parameters with a prism coupler, *Appl Opt* 12 (1973), 2901–2908.
2. A.C. Adams, D.P. Schinke, and C.D. Capiro, An evaluation of the prism coupler for measuring the thickness and refractive index of dielectric films on silicon substrates, *J Electrochem Soc* 126 (1979), 1539–1543.
3. T.W. Hou and C.J. Mogab, Plasma silicon oxide films on garnet substrates: Measurement of their thickness and refractive index by the prism coupling technique, *Appl Opt* 20 (1981), 3184–3188.
4. T.-N. Ding and E. Garmire, Measuring refractive index and thickness of thin films: A new technique, *Appl Opt* 22 (1983), 3177–3181.
5. F. Gao, F. Jin, and R. Xing, A guided-mode method for measuring electro-optic coefficients of poled polymer waveguides, *SPIE* 2987 (1996), 304–308.
6. F. Gao, G. Du, Vannadeth, P. Zhang, and F. Lun, An efficient method for measuring the parameters of single-mode anisotropic slab waveguides using the prism coupling technique, *Microwave Opt Technol Lett* 47 (2005), 575–580.
7. S. Yamamoto, Y. Koyamada, and T. Makimoto, Normal-mode analysis of anisotropic and gyrotropic thin-film waveguides for integrated optics, *J Appl Phys* 43 (1972), 5090–5097.
8. M. Born and E. Wolf, *Principles of optics*, Pergamon, New York, 1965.

© 2007 Wiley Periodicals, Inc.

COMPACT-PLANAR MONOPOLE LOOP ANTENNAS FOR 802.11b/g WLAN SYSTEMS

Mariusz Bledowski and Marek Kitlinski

Gdansk University of Technology, Gdansk, 80–952 Narutowicza 11/12, Poland

Received 7 February 2007

ABSTRACT: Two monopole antennas using Koch loop and Minkowski loop radiators fed by microstrip line are proposed for WLAN applications in the 2.45/5.25 bands. To achieve the desired resonances, new configurations of impedance transformer with transmission line length close to $\lambda/2$ were designed. The prototypes have been examined, fabricated, and experimentally tested and found to fulfill with excess WLAN system requirements. © 2007 Wiley Periodicals, Inc. *Microwave Opt Technol Lett* 49: 2299–2303, 2007; Published online in Wiley InterScience (www.interscience.wiley.com). DOI 10.1002/mop.22720

Key words: fractal; Minkowski loop; Koch loop

1. INTRODUCTION

In recent years, strong development of multiband wireless networks has sparked the need of new types of antennas for use at base stations, mobile computers (laptop), or mobile terminals. Today, the most widespread wireless local area network (WLAN) has increased the demand for compact, possibly omnidirectional planar antennas, working in two dedicated bands: 2.45 GHz (2.4–2.4835 GHz) and 5.25 GHz (5.15–5.35 GHz), for IEEE 802.11b/g. Therefore, advanced techniques of band allocation have to be developed, which would comply with the miniaturization demands. For this purpose, some dual-band and wideband printed monopole antennas have been reported [1–5]. The antenna in [1–3] uses a microstrip-fed printed monopole antenna, which radiates

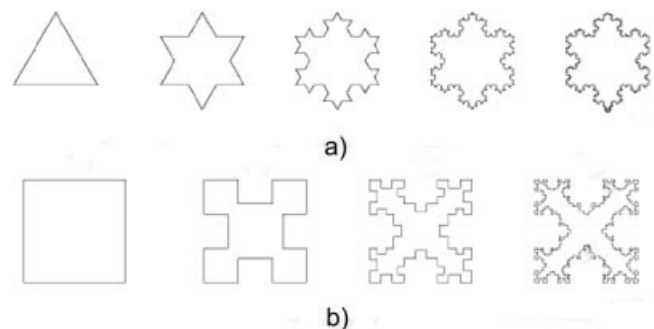


Figure 1 Generation of (a) Koch loop and (b) Minkowski loop